



CHORUS

This is the accepted manuscript made available via CHORUS. The article has been published as:

Pressure-induced structural transition in copper pyrazine dinitrate and implications for quantum magnetism

K. R. O'Neal, J. Zhou, J. G. Cherian, M. M. Turnbull, C. P. Landee, P. Jena, Z. Liu, and J. L. Musfeldt

Phys. Rev. B **93**, 104409 — Published 10 March 2016

DOI: [10.1103/PhysRevB.93.104409](https://doi.org/10.1103/PhysRevB.93.104409)

Pressure-induced structural transition in copper pyrazine dinitrate and implications for quantum magnetism

K. R. O’Neal,¹ J. Zhou,² J. G. Cherian,¹ M. M. Turnbull,³
C. P. Landee,³ P. Jena,² Z. Liu,⁴ and J. L. Musfeldt¹

¹*Department of Chemistry, University of Tennessee, Knoxville, Tennessee 37996, USA*

²*Department of Physics, Virginia Commonwealth University, Richmond, Virginia 23284, USA*

³*Department of Physics and Carlson School of Chemistry,
Clark University, Worcester, Massachusetts 01610, USA*

⁴*Geophysical Laboratory, Carnegie Institution of Washington, Washington D.C. 20015, USA*

(Dated: February 8, 2016)

We combined synchrotron-based infrared and Raman spectroscopies, diamond anvil cell techniques, and first principles calculations to unveil pressure-induced distortions in quasi-one-dimensional $\text{Cu}(\text{pyz})(\text{NO}_3)_2$. The crossover at 0.7 GPa is local in nature whereas the transition at 5 GPa lowers symmetry from $Pmna$ to $P222_1$ and is predicted to slightly increase magnetic dimensionality. Comparison with prior magneto-infrared results reveals the striking role of out-of-plane bending of the pyrazine ligand, a finding that we discuss in terms of the possibility of using pressure to bias the magnetic quantum critical transition in this classic $S = 1/2$ antiferromagnet.

PACS numbers: 62.50.-p, 78.30.-j, 75.50.Xx, 75.10.pq

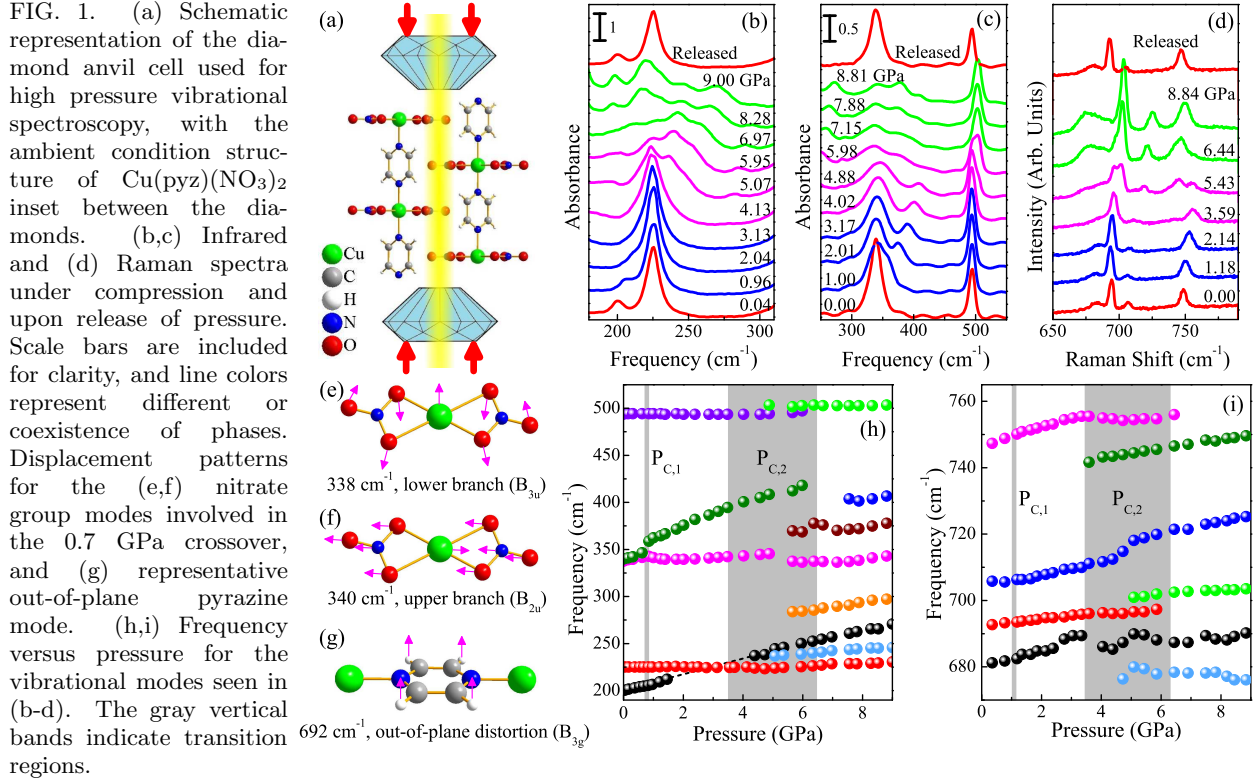
One of the fundamental challenges in functional magnetism is to understand quantum phase transitions, a classic example of which is the crossover from the antiferromagnetic to the fully polarized state [1–5]. Standard approaches to this problem often take advantage of molecule-based magnetic materials which are well-known to display overall low energy scales, complex phase diagrams due to competing interactions, and soft lattices [6–11]. One consequence is that small perturbations by an external stimulus can drive out-sized property changes. Copper pyrazine dinitrate, $\text{Cu}(\text{C}_4\text{N}_2\text{H}_4)(\text{NO}_3)_2$ or $\text{Cu}(\text{pyz})(\text{NO}_3)_2$, is a superb physical realization of an $S = 1/2$ quantum Heisenberg antiferromagnet, and as such, it has provided a platform for foundational investigations of quantum magnetism including magnetic quantum critical transitions, Tomonaga-Luttinger liquid behavior, and geometric frustration [12–21]. While copper pyrazine dinitrate has been widely studied over a range of temperatures and magnetic fields [18–25], almost nothing is known about the properties under pressure [26] despite evidence for spin-lattice coupling in applied magnetic field [21]. As we will show, this is because the critical pressure of $\text{Cu}(\text{pyz})(\text{NO}_3)_2$ is much higher than previously anticipated [26].

In this work, we bring together synchrotron-based infrared and Raman spectroscopies, diamond anvil cell techniques, and complementary first principles calculations to unveil spin-lattice coupling in $\text{Cu}(\text{pyz})(\text{NO}_3)_2$ under compression. We find critical pressures near 0.7 and 5 GPa that are related to nitrate group distortions and reduction of over-

all crystal symmetry from $Pmna$ to $P222_1$, respectively. The vibrational response of $\text{Cu}(\text{pyz})(\text{NO}_3)_2$ under compression also provides an opportunity to make a detailed comparison with prior magneto-infrared spectra [21] which reveal local lattice distortions through the quantum phase transition. Strikingly, we find that the out-of-plane pyrazine bending modes that red shift in applied magnetic field are a subset of those that break symmetry under pressure. This commonality provides enhanced opportunities for tuning the properties of this classic $S = 1/2$ antiferromagnet. Although spin-lattice mixing is most easily investigated in soft, low energy scale materials like $\text{Cu}(\text{pyz})(\text{NO}_3)_2$, similar energy transfer mechanisms are relevant in higher energy scale compounds.

Needle-shaped crystals of $\text{Cu}(\text{pyz})(\text{NO}_3)_2$ were grown as described previously [13]. A polycrystalline sample was loaded into a diamond anvil cell (Fig. 1(a)) either neat or with a pressure medium [27] and an annealed ruby ball [28]. Infrared measurements ($100\text{--}4000\text{ cm}^{-1}$; 1 cm^{-1} resolution, 300 K) employed the high brightness beam at the National Synchrotron Light Source at Brookhaven National Laboratory [29]. Raman scattering ($20\text{--}3260\text{ cm}^{-1}$; 0.5 cm^{-1} resolution, 300 K) was carried out with $\lambda = 532\text{ nm}$ at $<1\text{ mW}$ power. For both infrared and Raman spectra, compression is reversible within our sensitivity. Calculations of phase stability and lattice dynamics were carried out with spin-polarized density functional theory with the generalized gradient approximation [30] using the projector augmented wave method [31–33].

Figure 1(b,c) displays a close-up view of the low



frequency infrared spectra of copper pyrazine dinitrate under compression [33]. We track the mode frequencies versus pressure to identify structural transitions as indicated by mode splitting, abrupt frequency shifts, and the appearance or disappearance of various peaks. Examination of the frequency versus pressure trends (Fig. 1(h)) reveals two different transitions. The crossover at 0.7 GPa, designated here as $P_{C,1}$, is marked by the separation of the two nearly degenerate modes at 338 and 340 cm^{-1} that we assign as Cu-NO₃ counter-rotations and Cu-NO₃ shearing, respectively (Fig. 1(e,f)) [34]. The former has little interchain motion while the latter is a superior probe of interchain interactions. As pressure is applied the chains are forced together until the nitrate groups between the chains eventually come close together around $P_{C,1}$, hindering their interchain displacement. This explains why the upper branch hardens strongly ($\approx 11 \text{ cm}^{-1}/\text{GPa}$) whereas the lower branch is nearly unaffected.

Since the pyrazine rings are not involved in this transition, it should be anticipated that the magnetic properties will be unaffected. Indeed, susceptibility measurements up to 1.16 GPa show no sign of a crossover or change in exchange anisotropy [26]. This is quite different from other molecule-based magnets such as $\text{Co}[\text{N}(\text{CN})_2]_2$ [35]

and $\text{CuF}_2(\text{H}_2\text{O})_2(3\text{-chloropyridine})$ [36] that display pressure-induced magnetic crossovers near 1 GPa. The difference is due to the magnetic orbitals pointing along the chain direction in $\text{Cu}(\text{pyz})(\text{NO}_3)_2$ which is not modified through $P_{C,1}$. At the same time, examination of the C-H stretching modes (not shown) reveals no evidence for strengthened hydrogen bonding between the nitrate groups and pyrazine rings, so the rings must be rotating in order to allow the nitrate groups in the neighboring chains to move closer. A small ring rotation may explain the slight decrease in magnetic susceptibility above 0.75 GPa [9, 26]. No other infrared- or Raman-active vibrational modes are significantly modified through $P_{C,1}$ indicating that this crossover involves only nitrate groups and is local in nature.

Things are different at higher pressure where a second, more gradual process occurs between 3.5 and 6.5 GPa. This transition, henceforth called the 5 GPa transition and designated as $P_{C,2}$, is broader and associated with phase coexistence [33]. It also involves modes throughout the infrared and Raman spectra - consistent with a space group modification. For instance, nitrate group symmetry is reduced through this transition, as the 340 cm^{-1} Cu-NO₃ shearing mode is blocked and new modes appear (Fig. 1(h)). The pyrazine ring is also strongly af-

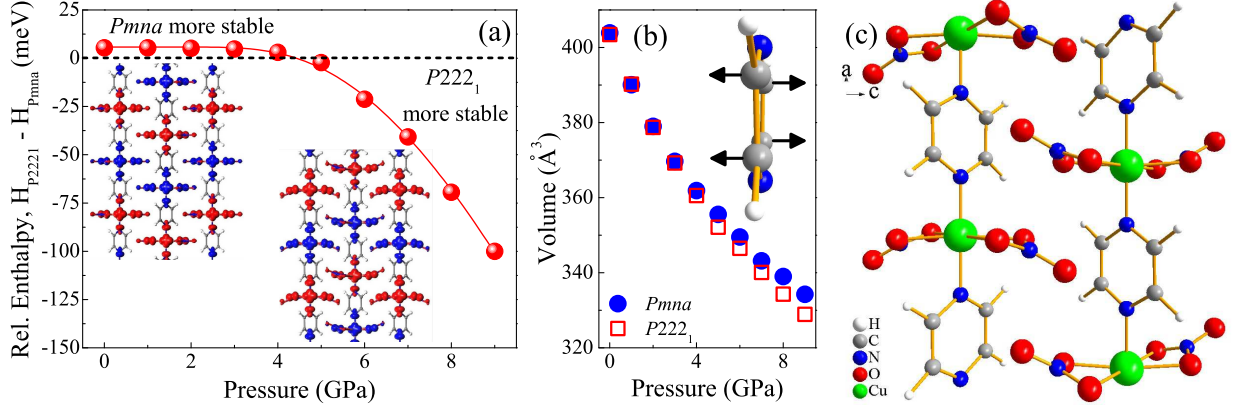


FIG. 2. (a) Relative enthalpy ($H = E + PV$) and (b) unit cell volume of the ambient $Pmna$ and high pressure $P222_1$ phases as a function of pressure. Insets in (a) are calculated magnetic isosurfaces where red and blue surfaces represent spin up and spin down states, respectively. The high pressure state is still a collinear antiferromagnet. The inset in (b) is the calculated high pressure distortions of the pyrazine ring in the indicated directions. (c) Predicted crystal structure of $\text{Cu}(\text{pyz})(\text{NO}_3)_2$ in the $P222_1$ space group at 10 GPa.

ected as exemplified by the out-of-plane C-H bending mode behavior (Fig. 1(d,g)). Overall there are more pyrazine-related vibrational modes observed in the high pressure phase, indicative of lower symmetry due to ring buckling. Cycling tests reveal that spectra before and after compression match very well demonstrating that these local lattice distortions are fully reversible when released from 9 GPa.

The crystal structure above $P_{C,2}$ will naturally be a subgroup of the ambient pressure $Pmna$ space group. [37] Since the pyrazine ring (which is aligned along a) buckles under compression, the symmetry along this axis should be lowered. The most likely subgroup candidates are $Pnc2$ and $P222_1$ as they have reduced a -axis symmetry compared to $Pmna$. In order to distinguish between these possibilities, we analyzed peak splitting as a function of pressure with particular focus on pyrazine ring and nitrate group behavior. The out-of-plane pyrazine ring distortions through $P_{C,2}$ clearly break symmetry along the a axis. The nitrate group also displays a new splitting pattern across the structural transition, as mentioned above. Inspection of the correlation table reveals that $Pnc2$ requires only symmetry lowering along a whereas $P222_1$ requires reduced symmetry in all three directions. The latter is therefore the more likely subgroup for the high pressure phase of $\text{Cu}(\text{pyz})_2(\text{NO}_3)_2$.

For additional tests of phase stability across the pressure-driven structural transition, we constructed models of several different phases of $\text{Cu}(\text{pyz})(\text{NO}_3)_2$ and performed structural optimizations at various pressures to determine unit cell enthalpy, volume, and magnetic properties [33]. These calculations

uncover two stable phases: $Pmna$ and $P222_1$. As shown in Fig. 2(a), the enthalpy of the $Pmna$ structure is lower than that of $P222_1$ at modest pressures, whereas $P222_1$ becomes more stable above ≈ 4.5 GPa. This transition pressure agrees very well with the experimentally determined $P_{C,2}$ near 5 GPa. Volume trends (Fig. 2(b)) are also consistent with a transition to $P222_1$ under compression. The predicted crystal structure in the high pressure $P222_1$ phase is shown in Fig. 2(c). Here, the chains shift $\approx 0.5 \text{ \AA}$ along the a axis, with neighboring chains moving in opposite directions. This brings the NO_3 groups closer together and forces them to bend out of plane (Fig. 2(c)), reducing symmetry in the bc plane. The pyrazine rings also display permanent out-of-plane distortions as shown in the inset of panel (b), although they are modest compared to the NO_3 bending. This leads to a symmetry reduction of the ring and thereby the a axis. The rings also have a small rotation about a , in line with the absence of strengthened hydrogen bonding under pressure.

Assuming that ring distortions and magnetic property changes are commensurate, we anticipate that the magnetic properties of $\text{Cu}(\text{pyz})(\text{NO}_3)_2$ will start to change only around 5 GPa. The pressure-induced out-of-plane ring distortions modify bond lengths and angles altering the magnetic orbital overlap and reducing J as t^2/U [21, 38] which, in turn, is expected to weaken intrachain antiferromagnetic ordering. Pressure effects on interchain coupling are, however, still unknown - although decreasing volume generally favors improved exchange interactions. That said, the absence of improved in-

terchain hydrogen bonding under pressure rules out any hydrogen bonding-driven magnetic exchange network dimensionality crossover of the type seen in $\text{CuF}_2(\text{H}_2\text{O})_2(\text{pyrazine})$ [26] or $\text{CuF}_2(\text{H}_2\text{O})_2(3\text{-chloropyridine})$ [36] - at least in this pressure regime. We therefore conclude that the overall trend in the 107 mK ordering temperature in $\text{Cu}(\text{pyz})(\text{NO}_3)_2$ [19] will depend upon the relative importance of ring distortion vs. volume effects. As a point of comparison, we note that pressure elevates T_N and T_C in several other molecule-based materials [35, 39–41]. In order to support these hypotheses, we used the calculated high pressure structure to predict the magnetic properties of the $P222_1$ phase. We find similar antiferromagnetic character as evidenced by the out-of-phase spin density pattern (insets, Fig. 2(a)).

One of the major advantages of materials like $\text{Cu}(\text{pyz})(\text{NO}_3)_2$ is their overall low energy scales compared to cuprates. From the magnetic properties point of view, these compounds can be saturated in experimentally available magnetic fields [6, 42, 43], providing a superb platform for the study of quantum phase transitions. $\text{Cu}(\text{pyz})(\text{NO}_3)_2$ is well known to display a magnetic quantum critical transition at 15 T [18]. Here, applied field drives an antiferromagnetic \rightarrow fully polarized state transition that is facilitated by spin-lattice interactions (which lower J_{AFM} and help to stabilize the fully polarized state) [21, 44].

What links the high pressure work presented here with prior magneto-infrared spectroscopy [21] is the fact that the modes which couple to the field-driven quantum critical transition are the same out-of-plane pyrazine bends that are involved in the 5 GPa structural transition. Figure 3 summarizes this behavior. This similarity is interesting because of the different coupling mechanisms: pressure acts directly on bond lengths and angles to tune magnetism [38] whereas spin-lattice coupling across the magnetic quantum critical transition relies on spin-orbit effects to link structure and magnetism. As shown in Fig. 3(a), the out-of-plane bending modes soften through the 15 T transition. The size of this simple red-shift follows the square of the magnetization [21] - a clear signature of spin-lattice coupling. Pressure is different. The N out-of-plane bending mode near 490 cm^{-1} splits under pressure, with one branch diminishing while the other grows. Moreover, the cluster of peaks centered near 810 cm^{-1} (assigned as H out-of-plane bends on the ring) blue shift and split into a five-fold multiplet. We conclude that while softening of the out-of-plane ring bends under applied field is small, symmetry is significantly lowered under compression.

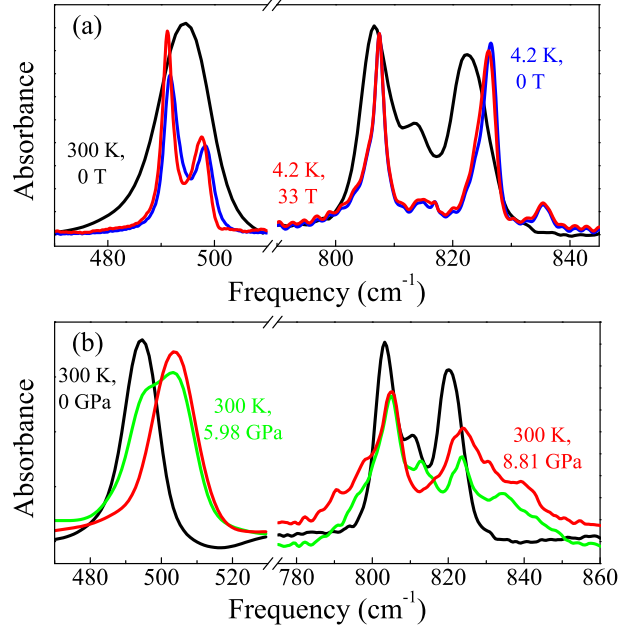


FIG. 3. Close-up views of the infrared response of $\text{Cu}(\text{pyz})(\text{NO}_3)_2$ in the vicinity of the infrared-active pyrazine ring out-of-plane distortion modes. Panel (a) summarizes the magnetic field-driven changes in these modes (reproduced from Ref. [21]), and (b) brings together complementary high pressure spectra. The conditions for each spectrum are indicated by labels with matching colors.

What is fascinating is that both types of external stimuli modulate the out-of-plane pyrazine displacements in $\text{Cu}(\text{pyz})(\text{NO}_3)_2$. It is well known that the pyrazine ring mediates magnetic exchange between copper centers [18], so there may be interesting opportunities to link the mechanisms of magnetic field and pressure driven transitions in this $S = 1/2$ Heisenberg antiferromagnet. The commonality of key displacement patterns under different types of physical tuning, revealed here for the first time in copper pyrazine dinitrate, may be present in other molecule-based materials and is associated with the presence of soft ligands that act as superexchange pathways. In fact, recent work by Ghannadzadeh *et al.* demonstrates that magnetic dimensionality and even the critical field is tunable under pressure in a chemically-similar molecule-based magnet that also incorporates pyrazine ligands [26]. This suggests that pressure may be able to bias the quantum phase transition in $\text{Cu}(\text{pyz})(\text{NO}_3)_2$ as well.

In summary, we measured the vibrational properties of copper pyrazine dinitrate up to 9 GPa in order to explore local lattice distortions in a quasi-one-dimensional $S = 1/2$ quantum Heisenberg antiferro-

magnet. The structural transition centered at $P_{C,2} = 5$ GPa results in a lower symmetry space group ($P222_1$) under pressure. The energy scale for magnetic property changes is therefore much higher than previously explored. At the same time, comparison of the behavior of the pyrazine out-of-plane distortion modes under pressure to that under magnetic field reveals that incorporating soft ligands as magnetic superexchange pathways can lead to enhanced tunability. In addition to advancing the understanding of spin-lattice coupling in molecule-based materials, this work emphasizes the advantage of combining pressure and magnetic field to bias the properties of quantum magnets.

This research is funded by the National Science Foundation (DMR-1063880) and the Petroleum Research Fund (52052-ND10). The National Synchrotron Light Source at Brookhaven National Laboratory is supported by the US Department of Energy under Contracts DE-AC98-06CH10886 and DE-FG02-96ER45579. The use of U2A beamline is funded by COMPRES under NSF Cooperative Agreement EAR 11-57758 and CDAC (DE-FC03-03N00144). Resources of the National Energy Research Scientific Computing Center supported by the Office of Science of the U.S. Department of Energy under Contract DE-AC02-05CH11231 are also acknowledged.

-
- [1] S. Sachdev, *Nat. Phys.* **4**, 173 (2008).
 [2] I. A. Zaliznyak, *Nat. Mater.* **4**, 273 (2005).
 [3] N. Büttgen, H.-A. Krug von Nidda, W. Kraetschmer, A. Günther, S. Widmann, S. Riegg, A. Krimmel, and A. Loidl, *J. Low Temp. Phys.* **161**, 148 (2010).
 [4] S. Paschen and J. Lerrea J., *J. Phys. Soc. Japan* **83**, 061004 (2014).
 [5] V. Zapf, M. Jaime, and C. D. Batista, *Rev. Mod. Phys.* **86**, 56 3(2014).
 [6] P. A. Goddard, J. Singleton, P. Sengupta, R. D. McDonald, T. Lancaster, S. J. Blundell, F. L. Pratt, S. Cox, N. Harrison, J. L. Manson, H. I. Southerland, and J. A. Schlueter, *New J. Phys.* **10**, 083025 (2008).
 [7] Z. Honda, H. Asakawa, and K. Katsumata, *Phys. Rev. Lett.* **81**, 2566 (1998).
 [8] C. P. Landee and M. M. Turnbull, *Mol. Cryst. and Liq. Cryst.* **335**, 193 (1999).
 [9] J. L. Manson, S. H. Lapidus, P. W. Stephens, P. K. Peterson, K. E. Carreiro, H. I. Southerland, T. Lancaster, S. J. Blundell, A. J. Steele, P. A. Goddard, F. L. Pratt, J. Singleton, Y. Kohama, R. D. McDonald, R. E. Del Sesto, N. A. Smith, J. Bendix, S. A. Zvyagin, J. Kang, C. Lee, M.-H. Whangbo, V. S. Zapf, and A. Plonczak, *Inorg. Chem.* **50**, 5990 (2010).
 [10] T. V. Brinzari, P. Chen, Q.-C. Sun, J. Liu, L.-C. Tung, Y. Wang, J. A. Schlueter, J. Singleton, J. L. Manson, M.-H. Whangbo, A. P. Litvinchuk, and J. L. Musfeldt, *Phys. Rev. Lett.* **110**, 237202 (2013).
 [11] T. Lancaster, P. A. Goddard, S. J. Blundell, F. R. Foronda, S. Ghannadzadeh, J. J. Möller, P. J. Baker, F. L. Pratt, C. Baines, L. Huang, J. Wosnitza, R. D. McDonald, K. A. Modic, J. Singleton, C. V. Topping, T. A. W. Beale, F. Xiao, J. A. Schlueter, A. M. Barton, R. D. Cabrera, K. E. Carreiro, H. E. Tran, and J. L. Manson, *Phys. Rev. Lett.* **112**, 207201 (2014).
 [12] R. B. Griffiths, *Phys. Rev.* **133**, A768 (1964).
 [13] A. Santoro, A. D. Mighell, and C. W. Reimann, *Acta Cryst.* **B26**, 979 (1970).
 [14] M. B. Stone, D. H. Reich, C. Broholm, K. Lefmann, C. Rischel, C. P. Landee, and M.M. Turnbull, *Phys. Rev. Lett.* **91**, 037205 (2003).
 [15] H. Kühne, H.-H. Klauss, S. Grossjohann, W. Brenig, F. J. Litterst, A. P. Reyes, P. L. Kuhns, M. M. Turnbull, and C. P. Landee, *Phys. Rev. B* **80**, 045110 (2009).
 [16] H. Kühne, A. A. Zvyagin, M. Günther, A. P. Reyes, P. L. Kuhns, M. M. Turnbull, C. P. Landee, and H.-H. Klauss, *Phys. Rev. B* **83**, 100407 (2011).
 [17] Y. Kono, T. Sakakibara, C. P. Aoyama, C. Hotta, M. M. Turnbull, C. P. Landee, and Y. Takano, *Phys. Rev. Lett.* **114**, 037202 (2015).
 [18] P. R. Hammar, M. B. Stone, D. H. Reich, C. Broholm, P. J. Gibson, M. M. Turnbull, C. P. Landee, and M. Oshikawa, *Phys. Rev. B* **59**, 1008 (1999).
 [19] T. Lancaster, S. J. Blundell, M. L. Brooks, P. J. Baker, F. L. Pratt, J. L. Manson, C. P. Landee, and C. Baines, *Phys. Rev. B* **73**, 020410(R) (2006).
 [20] A. A. Validov, M. Ozerov, J. Wosnitza, S. A. Zvyagin, M. M. Turnbull, C. P. Landee, and G. B. Teitelbaum, *J. Phys.: Condens. Matter* **26**, 026003 (2014).
 [21] Ö. Günaydın-Şen, C. Lee, L. C. Tung, P. Chen, M. M. Turnbull, C. P. Landee, Y. J. Wang, M.-H. Whangbo, and J. L. Musfeldt, *Phys. Rev. B* **81**, 104307 (2010).
 [22] B. R. Jones, P. A. Varughese, I. Olejniczak, J. M. Pigos, J. L. Musfeldt, C. P. Landee, M. M. Turnbull, and G. L. Carr, *Chem. Mater.* **13**, 2127 (2001).
 [23] A. V. Sologubenko, K. Berggold, T. Lorenz, A. Rosch, E. Shimshoni, M. D. Phillips, and M. M. Turnbull, *Phys. Rev. Lett.* **98**, 107201 (2007).
 [24] J. Rorhkamp, M. D. Phillips, M. M. Turnbull, and T. Lorenz, *J. Phys. Conf. Ser.* **200**, 012169 (2010).
 [25] J. Jornet-Somoza, M. Deumal, M. A. Robb, C. P. Landee, M. M. Turnbull, R. Feyerherm, and J. J. Novoa, *Inorg. Chem.* **49**, 1750 (2010).
 [26] S. Ghannadzadeh, J. S. Möller, P. A. Goddard, T. Lancaster, F. Xiao, S. J. Blundell, A. Maisuradze, R. Khasanov, J. L. Manson, S. W. Tozer, D. Graf, and J. A. Schlueter, *Phys. Rev. B* **87**, 241102(R) (2013).
 [27] Neat for Raman, vacuum grease for far infrared, and KBr for middle infrared. These media en-

- sure that the applied pressure is continuous, three-dimensional, and quasi-hydrostatic.
- [28] H. K. Mao, P. M. Bell, J. W. Shaner, and D. J. Steinberg, *J. Appl. Phys.* **49**, 3276 (1976).
 - [29] G. L. Carr, M. C. Martin, W. R. McKinney, K. Jordan, G. R. Neil, and G. P. Williams, *Nature* **420**, 153 (2002).
 - [30] J. P. Perdew, K. Burke, and M. Ernzerhof, *Phys. Rev. Lett.* **77**, 3865 (1996).
 - [31] P. E. Blöchl, *Phys. Rev. B* **50**, 17953 (1994).
 - [32] G. Kresse and J. Furthmüller, *Phys. Rev. B* **54**, 11169 (1996).
 - [33] See Supplemental Material for more details.
 - [34] P. M. Castro and P. W. Jagodzinski, *J. Phys. Chem.* **96**, 5296 (1992).
 - [35] C. J. Nutall, T. Takenobu, Y. Iwasa, and M. Kurmoo, *Mol. Cryst. and Liq. Cryst.* **343**, 227 (2000).
 - [36] K. R. O’Neal, T. V. Brinzari, J. B. Wright, C. Ma, S. Giri, J. A. Schlueter, Q. Wang, P. Jena, Z. Liu, and J. L. Musfeldt, *Sci. Rep.* **4**, 6054 (2014).
 - [37] This symmetry analysis assumes that the transition is second order.
 - [38] J. B. Goodenough, *Magnetism and the Chemical Bond* (Wiley, New York, 1963).
 - [39] J. J. Hamlin, B. R. Beckett, T. Tomita, J. S. Schilling, W. S. Tyree, and G. T. Yee, *Polyhedron* **22**, 2249 (2003).
 - [40] M. Mito, *J. Phys. Soc. Jpn.* **76**, 182 (2007).
 - [41] P. A. Quintero, D. Rajan, M. K. Peprah, T. V. Brinzari, R. S. Fishman, D. R. Talham, and M. W. Meisel, *Phys. Rev. B* **91**, 014439 (2015).
 - [42] A. Orendáčová, E. Čížmár, L. Sedláková, J. Hanko, M. Kajňáková, M. Orendáč, A. Feher, J. S. Xia, L. Yin, D. M. Pajerowski, M. W. Meisel, V. Zelenák, S. Zvyagin, and J. Wosnitza, *Phys. Rev. B* **80**, 144418 (2009).
 - [43] P. Vrábek, M. Orendáč, A. Orendáčová, E. Čížmár, R. Tarasenko, S. Zvyagin, J. Wosnitza, J. Prokleška, V. Sechovský, V. Pavlík, and S. Gao, *J. Phys.: Condens. Matter* **20**, 186003 (2013).
 - [44] J. L. Musfeldt, L. I. Vergara, T. V. Brinzari, C. Lee, L. C. Tung, J. Kang, Y. J. Wang, J. A. Schlueter, J. L. Manson, and M.-H. Whangbo, *Phys. Rev. Lett.* **103**, 157401 (2009).